Suggesting possible Functions of *GABRB3* and Establishing a Connection between *GABRB3* Absence and the Onset of Autism Spectrum Disorder

By: Cheryl Chang

Paul D. Schreiber High School

101 Campus Drive, Port Washington, NY, 11050

Table of Contents:

Acknowledgement:

Special thanks to my mentor for allowing me to conduct my own independent study under her, and to all those in my lab that helped guide me in adjusting to a lab environment and working with unfamiliar equipment. Also, special thanks to my lab for the resources they supplied for my study, and the opportunity they provided for me.

Thank you to my mom for establishing the initial connection for my summer research mentorship, and to all the teachers that assisted in proofreading my paper and providing feedback, especially my research teacher that never stopped supporting and believing in my research. Furthermore, thank you to my peers for their guidance throughout the research and application process.

Notation: *Research involving non-human vertebrates or human subjects was conducted under the supervision of an experienced teacher or researcher and followed state and federal regulatory guidance applicable to the humane and ethical conduct of such research.*

A. Research Rationale:

Autism Spectrum Disorders (ASD) is a neurodevelopmental disorder that negatively impacts communication and behavior; specifically it has been found to lead to impaired motor skills, sleeping disorders, and epilepsy (Mostofsky et al., 2009). Diagnosis for this disease averaged around 4 years of age, despite studies which have indicated that neural defects arise at even earlier developmental stages. Furthermore, early diagnosis and developmental intervention is believed to yield better clinical outcomes (Webb et al., 2014). However, behavioral manifestations of ASD symptoms as the primary mode of diagnosis has been shown to result in a delay of 3.6 years between when a parent initially contacts a health professional to the time the child receives a formal diagnosis (Crane et al., 2015). Thus, research towards developing mechanistic insight is especially valuable.

Over the years, research has implicated rare variants of *GABRB3* (subunit gene of GABAA receptor which encodes for subunit β3) to be associated with ASD, as increased *GABRB3* expression has been theorized to contribute to the pathogenesis of ASD (Sutcliffe et al., 2003 and Chen et al., 2014, respectively). One reason for *GABRB3*'s association with ASD is due to its location on chromosome 15q12, a prominent region of genomic DNA deletions and duplications commonly associated with ASD among other developmental disorders (Hogart et al., 2010). Additionally, it is believed that ASD and other behavioral defects may be caused by an imbalance between GABAergic inhibition and excitation leaning towards more excitation. Since GABA, Gamma-aminobutyric acid, is the primary inhibitory neurotransmitter present in the brain, GABAergic signaling during development may underlie ASD pathophysiology. (Chao et al., 2010, Hunt et al., 2012, Gant et al., 2009, Sutcliffe et al., 2003). Thus, further research regarding GABAergic signaling is necessary.

Furthermore, research has indicated that *GABRB3* induces abnormalities similar to symptoms of ASD. One study illustrated that mice without the *GABRB3* gene expressed the epilepsy phenotype in addition to behavioral abnormalities, including deficits in learning and memory, poor motor skills, and a disturbed rest-activity cycle (DeLorey et al., 1998). Another study done by DeLorey et al. showed that *GABRB3* deficient mice demonstrated various neurochemical, electrophysiological, and behavioral abnormalities similar to traits associated with ASD (DeLorey et al., 2005). Furthermore, in a followup study, DeLorey et al. discovered that *GABRB3* deficient mice manifested impaired social and exploratory behaviors among other indicators which establish that the phenotype of *GABRB3* deficient mice to be a potential representative model of ASD (Delorey et al., 2008).

This study seeks to build on the existing literature and reveal the effects *GABRB3* on neurotransmission in specific regions within the brain. One region that is of particular interest is the corpus callosum as it is primary mode of connection between the left and right cerebral hemispheres of the brain (**Figure A-1**). Specifically, the corpus callosum functions to integrate and transfer information from both hemispheres in order to process sensory, motor, and high-level cognitive signals (Goldstein et al., 2019). Additionally, it plays a major role in transferring visual, auditory, and somatosensory information in posterior regions (Goldstein et al., 2019). In regards to ASD, studies have established that the corpus callosum provides an inhibitory effect that normally deters uncoordinated hand-motor behavior, a common symptom expressed in patients with ASD (Tzourio-Mazoyer et al., 2016). Thus through investigating the effect *GABRB3* on intracortical communication, this study aims to discover if the presence or complete absence of *GABRB3* may play a role in inducing abnormalities in neuron transmission across the corpus callosum.

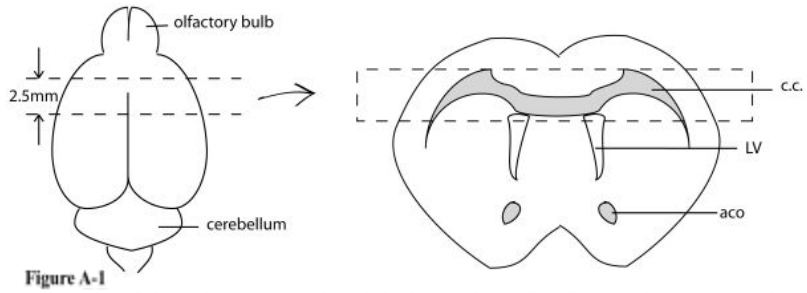

Figure A-1

The left image is a mouse brain and the bottom dashed line illustrates the coronal cut this experiment focused on, (7.5 mm away from the edge of olfactory bulb). The right image represents the brain section of the left. The tissue within the dashed rectangle highlights the corpus callosum. For this study, the lateral ventricle was used as a placement indicator for the slices of each brain imaged.

[CC – corpus callosum; LV – lateral ventricle; aca – anterior commissure]

(Zhang et al., 2012)

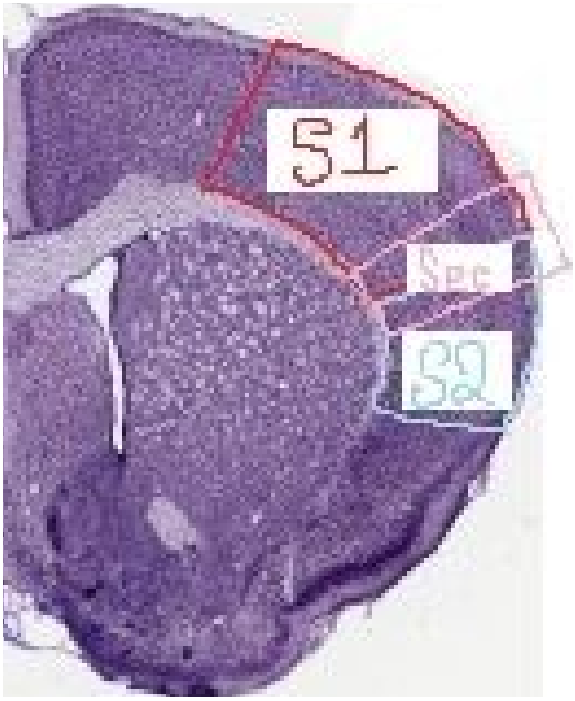

Figure A-2

The image above depicts the area of the primary and secondary somatosensory cortex and the slice that was imaged for this study. Outlined in red is the primary somatosensory cortex (S1) and outlined in blue is the secondary somatosensory cortex (S2). The slice image is outline in pink and contains the border between S1 and S2.

[S1 = primary somatosensory cortex, S2 = secondary somatosensory cortex, Sec = section imaged]

(Mikula et al. - edits by researcher)

The second region I chose to investigate was the border between the primary somatosensory cortex (S1) and the secondary somatosensory cortex (S2) (**Figure A-2**). The function of S1 ranges from processing incoming sensory input to the integration of both sensory and motor signals required for skilled movement. Throughout the years, numerous studies have illustrated a relationship between abnormal S1

activity, specifically the processing of somatosensory information, and motor dysfunction, similar to those expressed in those diagnosed with ASD (Elbert et al., 1998; Jacobs et al., 2012; Konczak and Abbruzzese, 2013). Furthermore, emerging research indicates that inaccurate processing and translation of sensory inputs contributes to deficits observed in neurological disorders, similar to ASD, which are characterized by imparied motor functions (Hummelsheim et al., 1988; Rub et al., 2003; Wolpert et al., 2013). S2 is a region whose functions remain largely unknown, however, a recent study indicates that there is a link present between the perception and processing of touch and S2 activation (Lamp et al., 2019). While Lamp et al. did not look exclusively on the effect of tactile stimulation of S2 activation, their results suggest that the S2 plays an important role in sense perception in that the S2 region was activated for both right and left hand tactile stimulation (Lamp et al., 2019). Thus the border between the two somatosensory cortices is of special interest.

B. Methodology:

B.1 Experiment Overview

The two groups used in this study was experimental, in which the mice had been bred to have an absence of the *GABRB3* gene, and the control, which was negative for *GABRB3* gene knockout. Afterwards, an *In Utero* electroporation took place on the 15th day after fertilization (E15.5 since mice breed at night) in the right cortical hemisphere in order to electroplate a DNA construct, Green fluorescent protein (GFP), and to knockout the *GABRB3* gene in most GABAergic cells (which are mainly inhibitory neurons) that preferentially occupy superficial layers of the somatosensory cortex, as they make up the majority of the cells born on E15.5 (Pla et al, 2006). No further injections were done after electroporation and the mice were maintained in a constant environment until postnatal day (P) 14. The animal was humanely sacrificed on P14 in order to analyze the effect of *GABRB3* gene deprivation in interneuron activity in a still developing neocortex.

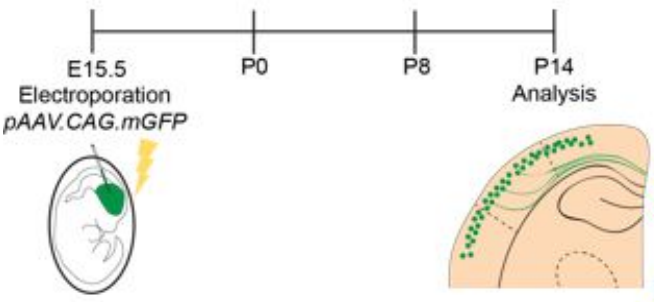

Figure B-1

The image above illustrates a timeline of the electroplating that took place in both the mutant and control mice, and the control gene (pAAV.CAG.mGFP) that was mechanically injected. The highlighted area, in green, of the embryonic mouse indicates the area of concentration for the electroplating, specifically the somatosensory cortex in the right cortical hemisphere. The electroplation took place at embryonic day (E) 15.5, and the mouse was sacrificed for analysis on postnatal day (P) 14. The image on the right illustrates the expected movement and migrations of the electroplated cells.

(Babij, 2019 [in preparation for future publication])

This experiment was initially a double blind study in which all of the data analysis was conducted without knowledge of whether the slide belonged to the experimental group or the control. The slides were not revealed to be either mutant or control until after the completion of data collection and analysis.

B.2 Immunohistochemistry [Cell Staining]

Taking advantage of the relationship between antigens and antibodies, in that antibodies bind only to specific corresponding antigens, immunohistory (IHC) is utilized to help visualize the distribution of cellular components in tissue, and in our case, visualize interneuron activity in both the corpus callosum and S1-S2 border. Essentially, IHC is used to stain specific cells to be viewed under the microscope. Staining is important as it is crucial to the identification and differentiation of one gene from another.

IHC Protocol (Adapted from Immunohistochemistry (IHC) Fundamental Principle):

I. Tissue Preparation
    A. The tissue had been previously cryostated and prepared by a supervisor for her ongoing experiment and placed in the freezer.
II. Solution Preparation
    A. All solutions used for this process were either pre-prepared by a supervisor or pre-purchased.
III. Incubation after removal from freezer
    A. For incubation, the slides of tissue were kept at room temperature in a transparent enclosed humidified chamber (which was achieved by placing a wet paper towel below the slides and elevating the slides above the wet paper towel using a cut plastic pipette such that the two would not touch).
    B. The slides were left in this condition for approximately 30 minutes to ensure that the tissue fully thawed out/defrosted.
IV. Rinsing the slides
    A. A phosphate buffer solution (PBS) with 0.025% Triton X-100 was used to rinse the slides.

B. The slides were rinsed by soaking the slides in PBS and allowing them to sit for 2 minutes at room temperature (with an aluminum cover to prevent overexposure to the light) before the solution was drained.
    1. This step was repeated 3 times.

V. Blocking the slides
    A. Blocking was achieved by pipetting serum from the same species as a secondary antibody
        1. The blocking serum was pre-purchased from a certified laboratory supplier.
    B. After the serum was evenly distributed throughout the tissue, an aluminum cover was placed over it and it was allowed to sit at room temperature for an hour before the blocking solution was drained
        1. The reason for this is because allowing it to sit in the solution for more than an hour would result in excessive blocking.
        2. This was a crucial step as blocking significantly lowers the chances of obtaining false positive results that may occur when the residual sites on the cryostat tissue binds to secondary antibodies.

VI. Applying the Primary
    A. Before applying anything, the slides were rinsed again (3x) to ensure that no blocking solution lingered on the slides.
    B. A primary was applied onto the slides and the slides were transported to the freezer (approx. 10°C) and allowed to incubate overnight
        1. This allows for the optimal binding of the antibodies to tissue targets to in turn reduce nonspecific background staining.

VII. Applying the Secondary
    A. Before applying the secondary, the primary was drained from the slides and they were rinsed (3x) to ensure that no primary solution remained.
    B. A fluorophore-conjugated secondary antibody was applied to the slides and the slides were allowed to incubate for 1 hour at room temperature (with an aluminum cover).

VIII. Preparing the slide for microscopy

A. In order to ensure that the stained tissue is protected against accidental exposure to other chemicals or weathering, a coverslip was placed on top of the slide and sealed with nailpolish (along the edges).

B.3 Confocal Microscopy [Imaging]:

After IHC is complete, imaging is achieved through utilizing a laser scanning confocal microscope (LSCM). As opposed to the conventional wide-field microscopy, confocal microscopy allows for Z-stacking, or the viewing of the three-dimensional structure of the specimen. If such a sample were to be viewed using wide-field imaging techniques, the image would lack contrast due to the present of fluorophores throughout the entire depth of the specimen being illuminated, and not simply at a specific depth. On the other hand, confocal microscopes collect light selectively from an optical section less than 1 μm thick at the plane of focus. Additionally, studies have confirmed that due to its capability of optical sectioning, confocal imaging is opportune for the study of cell structure and function using organic dyes, fluorescence in situ hybridization, and immunofluorescence reagents (Goldstein and Watkins, 2008 and Knoll et al., 2007). Hence confocal microscopy proved to be well matched for this experiment.

The two areas of the brain, I focused on were the corpus callosum and the border between the primary somatosensory cortex and secondary somatosensory cortex. I chose to image two slices per brain for a total of 12 brains, 24 photos, taking a 10x photo of the corpus callosum, 10x generalized photo of the S1-S2 border, and also a 20x photos laterally down the border (from the pia to the end of the somatosensory cortex). Due to the small field of view of the 20X images, they were taken in sections and later pieced together in the step detailed below.

All Confocal setup procedures undertaken were carried out in accordance to the laboratory's Confocal Setup protocol.

B.4 ImageJ: Fiji

Corpus Callosum

ImageJ, Fiji (a specific version of the software), was used in order to analyze the images taken by the confocal microscope. Data collected in this area dealt with the average thickness (using

layer 1 as a border in measurements of the left and the right, in addition to also taking a measurement of the middle) of the axons being projected through the corpus callosum from one hemisphere to the other. Specifically, using a measuring tool, the ratio between the actual size of the image and the pixels of it was established in order to allow for scaling and measuring of the imaged section. All data measurements taken in this assay was in micrometers and the average was determined by taking three measurements of the axonal projection, one through the middle of the axonal projection between the two hemispheres and the other two equidistant from it, layer 1 of the cortex as a border.

S1-S1 Border

Using this program, images of the latitudinal view of the S1-S2 border from the same brain was stitched together. This was a necessary step since images of this section were taken at 20X, which limited the field of view and did not allow for the imaging of the length of the S1-S2 border in one picture. Stitched pictures that resulted in crookedness were either retaken or had the edges cropped out, making for a slightly smaller width, which was later corrected for before beginning the data analysis.

For the S1-S2 border, I looked to analyze the percent of the imaged brain covered with axons, an indicator of interneuron activity between the S1 and S1 regions. This was accomplished through splitting the color channels and enhancing the amount of axons visible within the green channel [as the axons were visible due to the prenatal electroporation of green fluorescent protein]. Additionally, a cropping tool was used to exclude all non-somatosensory regions from consideration in order to increase the accuracy of the data collected.

B.5 Mice

The mice used in this sample were Postnatal (P) mice between P8-P12 years old and were sacrificed for an ongoing project, from which this stems as a side-study. Gender was mixed and not all the mice included in this experiment was from the same litter.

All procedures involved in handling and sacrificing the mice was acted in accordance with the Institutional Animal Care and Use Committee (**IACUC**) guidelines.

C. Results:

C.1 Overview

Data was collected and normalized by dividing the collected data by the number of electroplated cells (which had been previously found, prior to this experiment). Normalizing the data was important as it accounted for the variable of differing numbers of electroplated cells, as the amount of cells visible depended in part on the number of cells that had been successfully electroplated at E 15.5 (embryonic day 15). Specifically, normalization of the data was carried out by dividing either the axonal thickness in the corpus callosum assay or the percentage of area covered by excitatory neurons in the S1-S2 border assay, by the total number of cells successfully electroplated (which was taken from a previous study that focused on a different area of the somatosensory cortex and centered on a different hypothesis, that involved the same sample of cryostat brain slices). Furthermore, normalizing the data was crucial to revealing trends and significant in the data (**Fig C.1-1**).

Corpus Callosum				
Normalized; individ			Unnormalized; individ	
Ctrl	Mt		Ctrl	Mt
0.15503016	0.57485876		50.5398333	70
0.23371268	0.44067797		76.1903333	54
0.71598765	1.051875		77.3266667	90.226
0.67592593	1.1268447		73	80.402
1.54131373	1.30674667		78.607	64.646
1.3890915	1.27742		70.8436667	40.645
0.7744329	1.2711746		59.6313333	115.64
0.78412554	1.30485317		60.3776667	110.276
0.68699242	1.45461438		90.683	64.16
0.67089394	1.45065359		88.558	76.802
0.78510145			108.344	
0.78457246			108.271	
0.7664317	1.12597188		78.5310417	76.6797
0.3733829	0.34975659		18.0614172	23.5773636
0.03551773			0.83685744	

S1-S2 Border				
Individ Normalized			Individ Unnormalized	
Ctrl	Mt		Ctrl	Mt
0.008145	0.066934		2.655162	7.898265
0.024008	0.100307		7.826533	11.83621
0.02948	0.011853		3.183807	1.043056
0.026613	0.004526		2.874166	0.398313
0.087627	0.149417		4.468973	7.470858
0.101383	0.183597		5.170553	9.179842
0.056963	0.300724		4.386149	25.26082
0.051531	0.28557		3.96787	23.98791
0.094378	0.303667		12.45783	15.487
0.082475	0.30524		10.88665	15.56725
0.201242			27.77133	
0.160974			22.21441	
0.077068	0.171184		8.98862	11.81295
0.057937	0.122505		8.186967	8.459479
0.027939			0.436685	

Fig C.1-1: The charts above illustrate the difference in significance when the data is normalized versus when it is unnormalized, rationalizing the normalization for the data prior to any further tests of significance. The number in the highlighted box is the p-value resulting from a one-tailed t-test from the individual samples of the control and mutant values above. Note that the normalized individual data samples were significant, with p-value < 0.05, while the unnormalized data was not, with a p-value > 0.05.

To dispel any concerns over the significance of comparing the two different sections of the same brain and using them as "individual" data points in the data comparison, a t-test was conducted to find if there was any significant difference between the images taken at "Rhi" (when the lateral ventricle first begin to emerge) and "Bee" (when the lateral ventricles first diverge towards the

outside and produce an opening). The test found that the two distinct image sections from the same brain were neither significantly different for the mutants or the controls in either the corpus callosum or the S1-S2 border (**Fig C.1-2**).

Corpus Callosum			
Bee vs Rhi Mut. Normalized		Bee vs Rhi Ctrl. Normalized	
Rhi	Bee	Rhi	Bee
0.155030164	0.23371268	0.440677966	0.5748588
0.715987654	0.67592593	1.126844697	1.051875
1.541313725	1.3890915	1.27742	1.3067467
0.7744329	0.78412554	1.304853175	1.2711746
0.686992424	0.67089394	1.450653595	1.4546144
0.785101449	0.78457246		
0.776476386	0.75638701	1.120089886	1.1200899
0.44337713	0.3711739	0.396802466	0.3968025
0.923612663		0.961234155	

S1-S2 Border			
Bee vs Rhi Mut. Normalized		Bee vs Rhi Ctrl. Normalized	
Rhi	Bee	Rhi	Bee
0.02400777	0.008144669	0.10030685	0.066934449
0.026612649	0.029479697	0.00452629	0.011852908
0.101383389	0.087626931	0.18359684	0.149417163
0.051530778	0.05696298	0.28557037	0.300724036
0.082474592	0.094377527	0.30524022	0.30366657
0.160974002	0.201241511		
0.074497197	0.079638886	0.17584811	0.175848114
0.052219369	0.068131929	0.12639124	0.126391242
0.509072115		0.91234407	

Fig C.1-2: The data charts above illustrate the slim difference present between the data extracted from two distinct sections of the same brain, "Rhi" and "Bee", in both the mutant and the control groups for both the corpus callosum and the S1-S2 border. All possess very high P-values indicating that there is no significant difference present between the slices of the brain imaged.

C.2 Normalized individual comparison

Part of the Brain	Corpus Callosum		S1-S2 Border	
	Normalized; individ		Individ Normalized	
	Ctrl	Mt	Ctrl	Mt
	0.15503	0.574859	0.008145	0.066934
	0.233713	0.440678	0.024008	0.100307
	0.715988	1.051875	0.02948	0.011853
	0.675926	1.126845	0.026613	0.004526
	1.541314	1.306747	0.087627	0.149417
	1.389092	1.27742	0.101383	0.183597
	0.774433	1.271175	0.056963	0.300724
	0.784126	1.304853	0.051531	0.28557
	0.686992	1.454614	0.094378	0.303667
	0.670894	1.450654	0.082475	0.30524
	0.785101		0.201242	
	0.784572		0.160974	
Mean	0.766432	1.125972	0.077068	0.171184
SD	0.373383	0.349757	0.057937	0.122505
P-value	0.035518		0.027939	

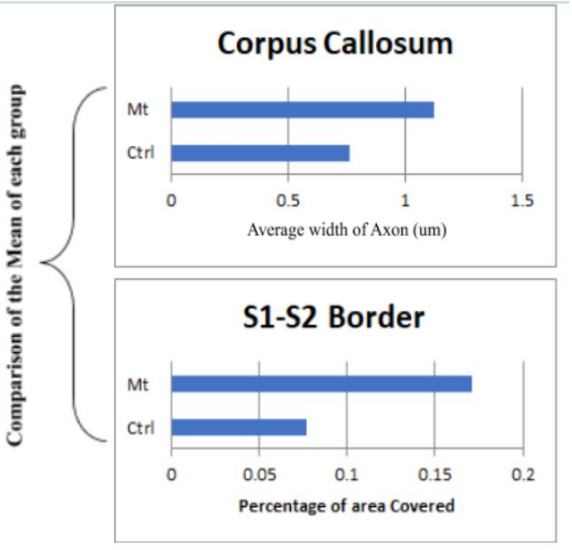

Fig C.2-1: In the Corpus Callosum assay, the difference between the axonal widths of the mutant group, in comparison to the control group, was significantly higher with a statistical significance of $p < 0.05$. In the S1-S2 border assays, the difference between the percentage of area covered by excitatory cells was also higher with a statistical significance of $p < 0.05$ in the mutant group, in comparison to the control group. Furthermore, the difference between the means of each assay is represented in the bar graphs to the right.

	Corpus Callosum			
	Bee Normalized		Rhi Normalized	
	Ctrl	Mt	Ctrl	Mt
	0.15503	0.57486	0.23371	0.44068
	0.71599	1.05188	0.67593	1.12684
	1.54131	1.30675	1.38909	1.27742
	0.77443	1.27117	0.78413	1.30485
	0.68699	1.45461	0.67089	1.45065
	0.7851		0.78457	
Mean	0.77648	1.13185	0.75639	1.12009
SD	0.44338	0.34308	0.37117	0.3968
P-value	0.17822		0.15106	

	S1-S2 Border			
	Bee Normalized		Rhi Normalized	
	Ctrl	Mt	Ctrl	Mt
	0.00814	0.06693	0.02401	0.10031
	0.02948	0.01185	0.02661	0.00453
	0.08763	0.14942	0.10138	0.1836
	0.05696	0.30072	0.05153	0.28557
	0.09438	0.30367	0.08247	0.30524
	0.20124		0.16097	
Mean	0.07964	0.16652	0.0745	0.17585
SD	0.06813	0.13318	0.05222	0.12639
P-value	0.19424		0.10484	

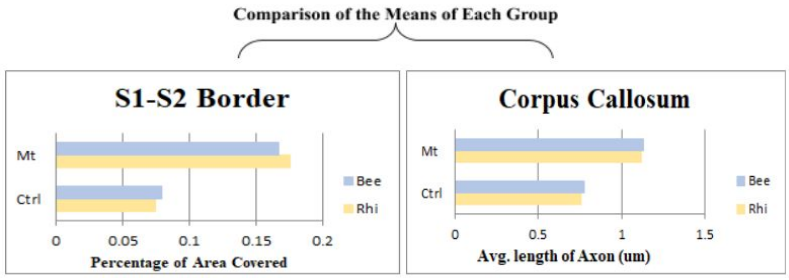

Fig C.2-2: Sorting based on the section that the image and data analysis was conducted, Rhi or Bee, both the corpus callosum and the S1-S2 border illustrated a trend in the difference between the mutant and the control. Furthermore, the difference between the averages of each assay is represented in the bar graphs above

C.3 Littermate Normalized Comparison

In the data analysis below, the samples were sorted based on litter and a paired t-test for significance was conducted in an attempt to further eliminate certain confounding variables, such as postnatal environment, maternal care, and littermate interactions. Specifically, there were a total of two available samples (one mutant, one control) for litter 3591, four samples (two mutant, two control) for litter 3594, and four samples (two mutant, two control) for litter 9157.

Part of the Brain	Corpus Callosum		
		Littermate; Norm	
		Ctrl	Mt
	3591	0.19437	0.50777
	3594	1.08058	1.19072
	9157	0.73189	1.37032
P-value		0.14806	

Fig C.3-1: The data above illustrates the Corpus Callosum data sorted via litter group and compared with a paired t-test. In both cases, the p-value indicates that the data is trending ($p < 0.2$).

Part of the Brain	S1-S2 Border		
		Litter mate; Norm	
		Ctrl	Mt
	3591	0.01608	0.08362
	3594	0.06128	0.08735
	9157	0.13477	0.2988
P-value		0.17037	

Fig C.3-2: The data above illustrates the S1-S2 border data sorted via litter group and compared with a paired t-test. In both cases, the p-value indicates that the data is trending ($p < 0.2$).

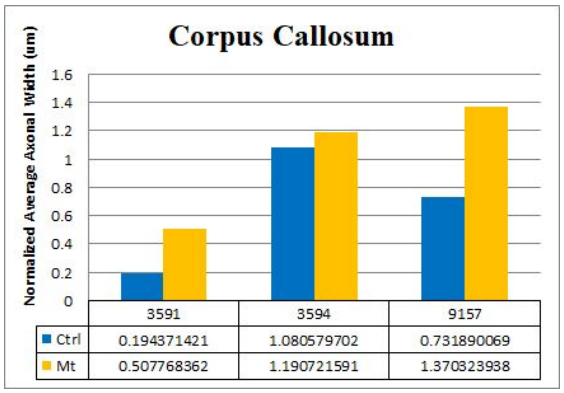

Fig C.3-3: This bar graphs illustrate the difference in means each litter group had with one another in regards to average axonal width (in um). As illustrated by the graph, the mutant group consistently showed a higher average.

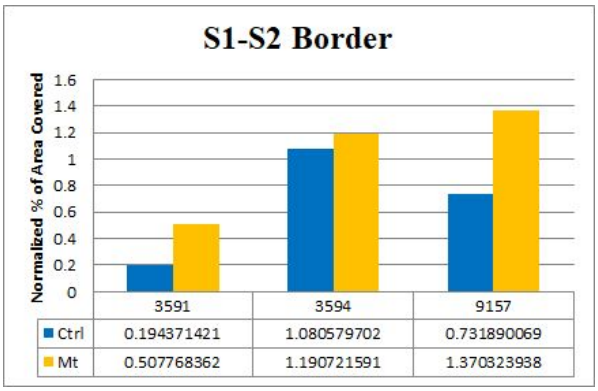

Fig C.3-4: This bar graphs illustrate the difference in means each litter group had with one another in regards to average percentage of area covered. As illustrated by the graph, the mutant group consistently showed a higher average.

C.4 Comparison of Confocal Images

The images below were taken using a confocal microscope (after immunohistochemical staining) and processed using a software called ImageJ (Schindelin et al., 2012). In all of the following images the activity and relative location of GABAergic neurons (which had been electroplated inserted a GFP gene) is visibly portrayed through the fluorescent green. Specifically, it was only the axons of the neurons that were injected with GFP and electroplated (to activate it's expression) that flourished beneath the microscope. While there exists room for error in the calculations extruded from the confocal images, as dendrite mass and cell bodies were not accounted for, because the conditions for analysis were constant between the mutant and control groups, possible errors resulting from the exclusion of dendritic and cell body analysis are noted but not specifically corrected for as there was both no means or strong reasons to do so.

In regards to the images, the white line at the top right of each image is a scale indicator for 100um and the images were all taken with a constant microscope setting.

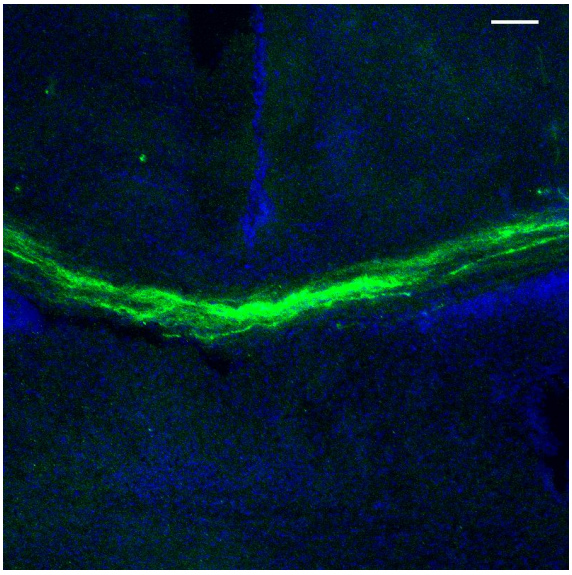

Fig C.4-1: The image above is a stitched image of subject 7 of litter 9157, which is negative for the knockout of the *GABRB3* gene and thus acted as a control in this experiment. It displays the axonal projection across the corpus callosum (in the green).

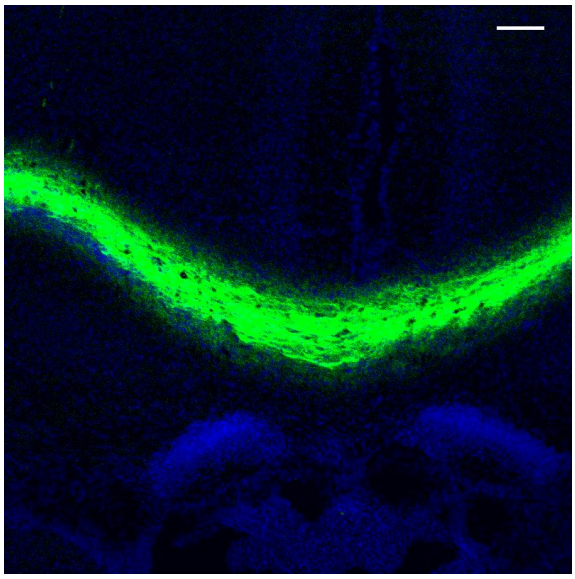

Fig C.4-2: The image above is a stitched image of subject 3 of litter 9157, which is positive for the knockout of the *GABRB3* gene and thus acted as a mutant in this experiment. It displays the axonal projection across the corpus callosum (in the green).

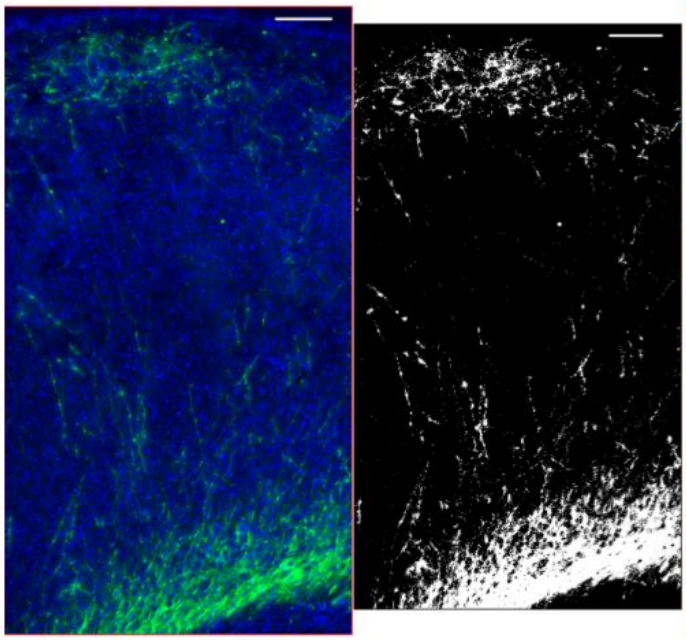

Fig C.4-3: The image on the left is a stitched image of subject 1 of litter 9157, which is negative for the knockout of the *GABRB3* gene and thus acted as a control in this experiment. It displays the axonal coverage in the S1-S2 border (in the green). The image on the right illustrates the same image in black and white, and with the axonal coverage in the S1-S2 border enhanced via ImageJ.

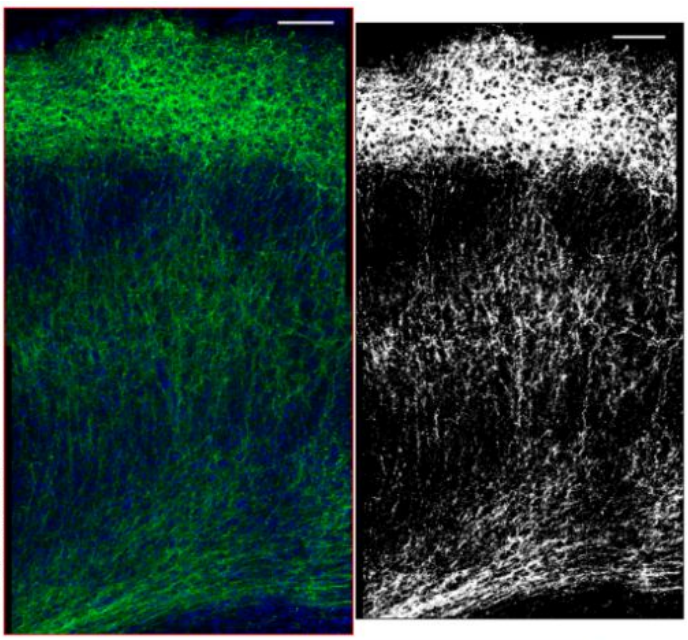

Fig C.4-4: The image on the left is a stitched image of subject 2 of litter 9157, which was positive for the knockout of the *GABRB3* gene and was thus part of the mutant group. It displays the axonal coverage in the S1-S2 border (in the green). The image on the right illustrates the same image in black and white, and with the axonal coverage in the S1-S2 border enhanced via ImageJ.

D. Analysis & Discussion

D.1 Corpus Callosum

Interestingly, the analysis showed that the thickness of the axonal projection across the corpus callosum to be significantly larger, with a P-value of less than 0.05, in the mutants, which had been deprived of the *GABRB3* gene, than the control when compared individually (**FigC2-1**). In regards to a comparison based on the slice of the brain imaged, there was a trending significance, with a P-value of less than 0.2 **(FigC2-1**). Littermate pairing revealed the same trending significance, using a paired t-test (**FigC3-1** and **FigC3-3**). Furthermore, there is also a notable visible difference in the thickness of the axonal projection through the corpus callosum between the mutants and the control **(FigC4-1** and **FigC4-2**).

As the *GABRB3* gene encodes for a prominent receptor subunit in GABAergic interneurons, an increase in average width of axonal projections with the absence of this gene indicates that there is either an increase in pyramidal neuron activity or a decrease in inhibitory neuron activity. Both scenarios reflect a possible defect in intra-cortical communication between the two hemispheres, specifically in the normal inhibitory effect provided by the corpus callosum that aids in deterring common ASD indicators, most notably uncontrollable motor behavior in the hands (Tzourio-Mazoyer et al., 2016). Thus these results suggest a link between the expression of the GABRB3 gene and the onset of ASD.

The applications of these results include a deeper mechanistic understanding of the role of *GABRB3* irregularities in inducing the onset of ASD and strengthens the belief that *GABRB3* defects are linked to ASD. Additionally, study reveals possible functions of *GABRB3* in the developing neocortex. For example, an increase in width of the axonal projections across the corpus callosum suggests that *GABRB3* may be essential to inhibitory neuron activity and/or proper pyramidal neuron expression, in addition to being involved in the specialization and filtration of intra-hemispheric communication.

D.2 S1-S2 Border

In regards to the S1-S2 border, the analysis illustrates that the percentage of area covered by the inhibitory neurons electroplated at E15.5 was significantly larger, with a P-value of less than 0.05, in the mutants, which had been deprived of the *GABRB3* gene, than the control when compared

individually (**FigC2-1**). In regards to a comparison based on the slice of the brain imaged, there was a trending significance, with a P-value of less than 0.2 (**FigC2-2**). Littermate pairing was analyzed using a paired t-test and revealed a trending significance (**FigC3-2** and **FigC3-4**). Furthermore, a drastic visible difference in the percentage of area covered by inhibitory neurons in the S1-S2 border, and in turn neuron activity in that region, can be found between the mutants and the control (**FigC4-3** and **FigC4-4**).

The significantly higher percentage of GABAergic neuron coverage in the mutant mice than in the control also works to strengthen the connection between irregular expression of the *GABRB3* gene and ASD. This is because abnormal neural activity in S1 has been indicated to induce dysfunctions similar to those expressed in those diagnosed in ASD patients (Elbert et al., 1998; Jacobs et al., 2012; Konczak and Abbruzzese, 2013; Hummelsheim et al., 1988; Rub et al., 2003; Wolpert et al., 2013). Additionally, while abnormal activity in the S2 region has not been connected to ASD, the S2 region has been indicated to play a crucial role in sense perception and as such abnormal activity in the S2 region may lead to a deficiency or overload of sense perception (Lamp et al., 2019). However, no definite conclusion can be drawn as this study looked at the S1-S2 border and not specifically at either somatosensory cortex.

Since the region observed was the S1-S2 border, an increased percentage of inhibitory neurons in the S1-S2 border of mutants suggests increased communication between the two cortices. This is of significance as it indicates the role of the *GABRB3* gene as a regulator in the amount of information that is to be communicated and shared between the two cortices. Without the presence of the gene, there was a notable decrease in the filtration of information between the two somatosensory cortices, as indicated by the increased presence of interneurons present. Thus, a possible function of *GABRB3* as a gene regulatory of inhibitory neuron activity.

E. Limitations and Future Research

A major limitation of this study is the time constraint which prevented a greater number of samples to be stained, imaged, and analyzed. Furthermore, it is impossible to control for every variable and variables including parent genes, environment during development, and parent or littermate interactions. While littermate pairing sought to resolve this problem, some litters resulted in only one mutant mice and others in no mutant mice, allowing for no comparison. Thus the samples used were not optimal. Additionally, the absence of a technique to selectively decrease or increase the concentration of the *GABRB3* gene, rather than the complete knockout of it, proves to be a suboptimal model of realistic occurrences. This is because it is very rare for the gene to be completely deleted in humans, whereas irregularities with the gene is moderately common.

Future research would include a greater number of samples and more emphasis on littermate pairing, as the results indicate a trending significance in the difference among littermate pairings with a p-value < 0.2. In addition, another area for future research would be to further unravel whether it is an increase in excitatory neuron activity or a decrease in inhibitory neuron activity that can be attributed to an irregularity in intra-cortical communication. One main area of future research would be the implication of these findings as a foundation to expand the current known functions of the *GABRB3* gene and possibly establish a new mode of testing for ASD that lowers the average age of diagnosis allowing for earlier, more efficient treatment. The current work leads to the promise of potentially developing more precise mechanistic insight into the onset of ASD, as well as discovering the importance, if any, of the *GABRB3* gene in early brain development.

Bibliography:

Andrej Stancak, Karsten Hoechstetter, Jaroslav Tintera, Jiri Vrana, Rosa Rachmanova, Jiri Kralik, Michael Scherg, Source activity in the human secondary somatosensory cortex depends on the size of corpus callosum, Brain Research,Volume 936, Issues 1–2, 2002, Pages 47-57

Chao, H.T., et al., *Dysfunction in GABA signalling mediates autism-like stereotypies and Rett syndrome phenotypes.*Nature, 2010. **468**(7321): p. 263-9.2.

Chen, C. H., Huang, C. C., Cheng, M. C., Chiu, Y. N., Tsai, W. C., Wu, Y. Y., … Gau, S. S. (2014). Genetic analysis of GABRB3 as a candidate gene of autism spectrum disorders. *Molecular autism*, *5*, 36. doi:10.1186/2040-2392-5-36

Crane, L., Chester, J. W., Goddard, L., Henry, L. A., & Hill, E. (2016). Experiences of autism diagnosis: A survey of over 1000 parents in the United Kingdom. Autism, 20(2), 153–162. https://doi.org/10.1177/1362361315573636

DeLorey TM, Handforth A, Anagnostaras SG, Homanics GE, Minassian BA, Asatourian A, Fanselow MS, Delgado-Escueta A, Ellison GD, Olsen RW. Mice lacking the beta3 subunit of the GABAA receptor have the epilepsy phenotype and many of the behavioral characteristics of Angelman syndrome. J Neurosci. 1998;18:8505–8514.

DeLorey TM. *GABRB3* gene deficient mice: a potential model of autism spectrum disorder. Int Rev Neurobiol. 2005;71:359–382.

DeLorey TM, Sahbaie P, Hashemi E, Homanics GE, Clark JD. GABRB3 gene deficient mice exhibit impaired social and exploratory behaviors, deficits in non-selective attention and hypoplasia of cerebellar vermal lobules: a potential model of autism spectrum disorder. Behav Brain Res. 2008;187:207–220.

Elbert T, Candia V, Altenmuller E, Rau H, Sterr A, Rockstroh B, Pantev C, Taub E. Alteration of digital representations in somatosensory cortex in focal hand dystonia. Neuroreport. 1998;9:3571–3575.

Gant, J.C., et al., *Decreased number of interneurons and increased seizures in neuropilin 2 deficient mice: implications for autism and epilepsy.*Epilepsia, 2009. **50**(4): p. 629-45

Goldstein A, Covington BP, Mesfin FB. Neuroanatomy, Corpus Callosum. [Updated 2019 Jun 28]. In: StatPearls [Internet]. Treasure Island (FL): StatPearls Publishing; 2019 Jan-. Available from: https://www.ncbi.nlm.nih.gov/books/NBK448209/

Han, S., et al., *Autistic-like behaviour in Scn1a+/-mice and rescue by enhanced GABA-mediated neurotransmission.*Nature, 2012. **489**(7416): p. 385-90.3.

Hogart A, Wu D, LaSalle JM, Schanen NC. The comorbidity of autism with the genomic disorders of chromosome 15q11.2-q13. Neurobiol Dis. 2010;38:181–191.

Hummelsheim H, Bianchetti M, Wiesendanger M, Wiesendanger R. Sensory inputs to the agranular motor fields: a comparison between precentral, supplementary-motor and premotor areas in the monkey. Exp. Brain Res. 1988;69:289–298.

Immunohistochemistry (IHC) Fundamental Principle, How IHC Works. (n.d.). Retrieved from;https://www.bosterbio.com/protocol-and-troubleshooting/immunohistochemistry-ihc-principle

Jacobs M, Premji A, Nelson AJ. Plasticity-inducing TMS protocols to investigate somatosensory control of hand function. Neural Plast. 2012;2012:350574

Konczak J, Abbruzzese G. Focal dystonia in musicians: linking motor symptoms to somatosensory dysfunction. Front. Hum. Neurosci. 2013;7:297.

Lamp Gemma, Goodin Peter, Palmer Susan, Low Essie, Barutchu Ayla, Carey Leeanne M., Activation of Bilateral Secondary Somatosensory Cortex With Right Hand Touch Stimulation: A Meta-Analysis of Functional Neuroimaging Studies, Frontiers in Neurology, Vol 9, 2019, pages 11-29

Mikula, Shawn. “Mus Musculus -> Nissl, Coronal, Histo, Whole-Brain, Adult.” *BRAINMAPS.ORG - BRAIN ATLAS, BRAIN MAPS, BRAIN STRUCTURE, NEUROINFORMATICS, BRAIN, STEREOTAXIC ATLAS, NEUROSCIENCE*, Brainmaps.org, www.brainmaps.org/index.php?action=viewslides&datid=38.

Mostofsky SH, Powell SK, Simmonds DJ, Goldberg MC, Caffo B, Pekar JJ. Decreased connectivity and cerebellar activity in autism during motor task performance. Brain. 2009;132:2413–2425. [PMC free article][PubMed] [Google Scholar] This is the largest fMRI study investigating the neural basis of basic motor function (finger tapping) in ASD, and the first to examine functional connectivity during a motor task.

Pla, Ramón, et al. “Layer Acquisition by Cortical GABAergic Interneurons Is Independent of Reelin Signaling.” *Journal of Neuroscience*, Society for Neuroscience, 28 June 2006, www.jneurosci.org/content/26/26/6924.

Rub U, Schultz C, Del Tredici K, Gierga K, Reifenberger G, de Vos RA, Seifried C, Braak H, Auburger G. Anatomically based guidelines for systematic investigation of the central somatosensory system and their application to a spinocerebellar ataxia type 2 (SCA2) patient. Neuropathol. Appl. Neurobiol. 2003;29:418–433.

Rueden, C. T.; Schindelin, J. & Hiner, M. C. et al. (2017), "ImageJ2: ImageJ for the next generation of scientific image data", *BMC Bioinformatics* **18:529**, PMID 29187165, doi:10.1186/s12859-017-1934-z (on Google Scholar).

Schindelin, J.; Arganda-Carreras, I. & Frise, E. et al. (2012), "Fiji: an open-source platform for biological-image analysis", *Nature methods* **9(7)**: 676-682, PMID 22743772, doi:10.1038/nmeth.2019 (on Google Scholar).

Sutcliffe JS, Nurmi EL, Lombroso PJ. Genetics of childhood disorders: XLVII. Autism, part 6: duplication and inherited susceptibility of chromosome 15q11-q13 genes in autism. J Am Acad Child Adolesc Psychiatry. 2003;42:253–256.

Tzourio-Mazoyer N. Intra- and Inter-hemispheric Connectivity Supporting Hemispheric Specialization. In: Kennedy H, Van Essen DC, Christen Y, editors. Micro-, Meso- and Macro-Connectomics of the Brain [Internet]. Springer; Cham (CH): Mar 11, 2016. pp. 129–146.

Webb, SJ, Jones, EJH, Kelly, J. (2014) The motivation for very early intervention for infants at high risk for autism spectrum disorders. International Journal of Speech and Language Pathology 16(1): 36–42.

Wolpert DM, Pearson KG, Ghez CPJ. The organization and planning of movement. In: Kandel ER, Schwartz JH, Jessell TM, Seigelbaum SA, Hudspeth AJ, editors. Principles of Neural Science. 5. New York: McGraw-Hill Companies; 2013. pp. 743–767.

Zhang, Lin & yu, wu & Schroedter, Ingo & Kong, Jiming & Vrontakis, Maria. (2012). Galanin Transgenic Mice with Elevated Circulating Galanin Levels Alleviate Demyelination in a Cuprizone-Induced MS Mouse Model. PloS one. 7. e33901. 10.1371/journal.pone.0033901.